International Journal of General Medicine Dovepress

Open Access Full Text Article ORIGINAL RESEARCH

Integrative Proteomics and Phosphoproteomics Profiling of Symptomatic Accessory Navicular Bone Based on Tandem Mass Tag Technology

Bin Liu*, Ran Wei*, Yuqing Wang, Zishen Cheng, Liangliang Jiang, Xiaopeng Pu, Yaxing Zhang, Yantao Wang, Qiangjun Kang

Department of Orthopaedics, Bethune International Peace Hospital, Shijiazhuang, 050082, China

*These authors contributed equally to this work

Correspondence: Qiangjun Kang, Department of Orthopaedics, Bethune International Peace Hospital, No. 398, Zhongshan Road, Qiaoxi District, Shijiazhuang, Hebei, 050082, China, Email 19933000561@163.com

Background: The accessory navicular bone (ANB) is a common accessory bone in the foot. Certain ANBs significantly impair patients' feet normal walking function. Foot injury is associated with ANB after athletic training. However, the molecular mechanism of foot injury with ANB after athletic training remains unclear. This study aims to investigate the proteomics and phosphoproteomics profile of foot injury with the ANB after athletic training.

Patients and Methods: We collected ANB tissues and normal bone (NB) tissues from 5 foot injury patients with ANB after 3 months of athletic training to perform proteome sequencing by tandem mass tag (TMT) technology. Then, the differentially expressed proteins (DEPs) and phosphorylation proteins (DPPs) were identified between the ANB and NB groups. Furthermore, the potential functions of DEPs and DPPs were annotated, respectively. Besides, the protein-protein interaction (PPI) network was constructed for DEPs.

Results: A total of 147 DEPs (129 upregulated and 18 downregulated) were detected. Functional enrichment suggested that they were involved in extracellular matrix (ECM)-receptor interaction and cell adhesion. PPI network showed that COL4A1 and COL4A2 had the highest interaction score, followed by RBBP4 and RBBP7. In addition, phosphoproteomics analysis identified 4 upregulated and 1 downregulated DPPs, and they were primarily enriched in regulating lipolysis in adipocytes.

Conclusion: Our study found that foot injury with ANB after exercise training may be associated with proteins related to inflammation and immunity (such as MRC1, UBE2N, CYCS), bone repair and regeneration (such as Emilin2, COL4A1, COL4A2, and ITGA9), and bone microstructure homeostasis (such as GCA and ANXA3). This provides new insights into understanding its pathogenesis and guiding treatment strategies.

Keywords: accessory navicular bone, athletic training, proteomics, phosphoproteomics

Introduction

The accessory navicular bone (ANB) is an excrescent ossicle that exists in the interior of the tarsal navicular bone and presents in 10% to 14% of normal feet.[1–3] It is a variant of the navicular tuberosity caused by incomplete fusion of its secondary ossification center.[2] The clinical manifestations of ANB are mainly pain or tenderness, which is attributed to the abnormal insertion of the posterior tibial tendon into ANB, altering tendon leverage and disrupting the normal biomechanical function of the arch.[4] It can be classified into 3 types: Type I is a small accessory bone within the substance of the posterior tibial tendon, without attachment to the body of the navicular; type II is an ANB with a synchondrosis that has the appearance of a cartilaginous unit containing islands of hyaline and fibrocartilage, which is divided into a and b types according to the angle of ANB and scaphoid tuberosity; and type III is a corneal navicular that probably represents an end stage of type II.[5–7] Most of the symptomatic cases are type II ANB.[8] Some patients showed

Received: 25 June 2024
Accepted: 1 December 2024
Published: 14 December 2024

local uplift and tenderness at the navicular tubercle, which seriously affected the normal walking function of the foot.[9] Wang et al reported that patients with ANB appeared to have foot pain and (or) limited activity after 3 months of athletic training and had certain influences on athletic training.[10] However, the underlying molecular mechanisms of foot injury with ANB after athletic training remain unclear.

The proteome is all corresponding proteins expressed by the genome of a cell or a tissue.[11] Proteomics takes the proteome as the research object and understands the laws of life activities from the overall protein level.[12] Currently, proteomic methods have been widely used to explore the pathology of bone related diseases, including osteoporosis,[13] osteosarcoma,[14,15] osteoarthritis,[16,17] and fractures.[18,19] Tandem mass tag (TMT) technology, as a classic mass spectrometry quantitative method in proteomics studies, not only identified the abundance of protein, but also helped us to find biomarkers and understand the pathogenesis of diseases.[20,21] Liang et al reported that TMT technology is a feasible approach to identifying the potential therapeutic targets in primary type I osteoporosis treated with qianggu decoction.[22] Huang et al used TMT proteomics technology to reveal the differences in extracellular vesicle proteome in different types of inflammatory arthritis, and screened potential biomarkers and possible molecular mechanisms.[16]

Protein phosphorylation is a common regulation mode that affects almost all biological processes.[23] Serine, threonine, and tyrosine are the most common phosphorylation modification sites.[24] Protein phosphorylation plays a role in bone formation.[25] A study based on phosphogenomics found that serine/threonine protein kinase D1 activates the pro-osteogenic transcription factor RUNX2 by triggering the phosphorylation and nuclear exclusion of histone deacetylase HDAC7 in the early stages of osteoblast formation.[26] In bone tissues, cyclic adenosine monophosphate (cAMP) related protein phosphorylation and protein kinase A (PKA) activation could trigger the cascaded expression of osteogenesis-related genes.[27] So far, little is known about protein abundance and phosphorylation profiles in patients with ANB in the foot after athletic training.

In this study, we investigated the differentially expressed proteins (DEPs) and phosphorylation proteins (DPPs) between ANB and normal bone (NB) by TMT technology to explore the critical proteins related to foot injury with ANB after 3 months of athletic training. We hope to provide new insights into the pathogenesis of ANB injury.

Materials and Methods

Source of Samples

In this study, we collected ANB tissue and normal bone tissue from 5 foot injury patients who had undergone 3 months of exercise training and exhibited clinical manifestations of ANB. All patients met the surgical criteria: i) Patients who have received formal conservative treatment for more than 6 months have not shown significant improvement in medial foot pain; ii) X-ray images of patients showed obvious pseudarthrosis formation and larger ANB; iii) There were obvious abnormal protrusion on the medial foot, skin redness and swelling, accompanied by obvious tenderness of the posterior tibial tendon. The age of the patients ranged from 21 to 32 years old, and their disease duration varied from 11 to 24 months. The foot anatomy diagram, including 3 subtypes diagram, had been provided in Figure 1. According to the ANB subtype classification, all patients in this study were classified as type II ANB, with three on the right foot and two on the left foot. The clinical data of the patients are provided in detail in Table 1. This study was performed according to the Declaration of Helsinki and approved by the Ethics Committee of Bethune International Peace Hospital (NO. 2023-KY -187). Patients' informed consent was obtained.

Protein Extraction

Each sample was ground to a powder in liquid nitrogen. Lysis buffer (2M thiourea (Bio-Rad, USA), 7M Urea (Sigma-Aldrich, USA), 1‰ CHAPS (Bio-Rad, USA)) was added. Then, the samples were left on ice for 20 min, centrifuged at 13,000 rpm for 20 min at 4 °C, and the supernatant was stored at − 80°C for further proteomics analysis. Bradford assay (Thermo Fisher Scientific, USA) was used to determine the protein concentration. The sodium dodecyl sulfate-polyacrylamide gel electrophoresis (SDS-PAGE) was used to detect the quality of sample proteins.

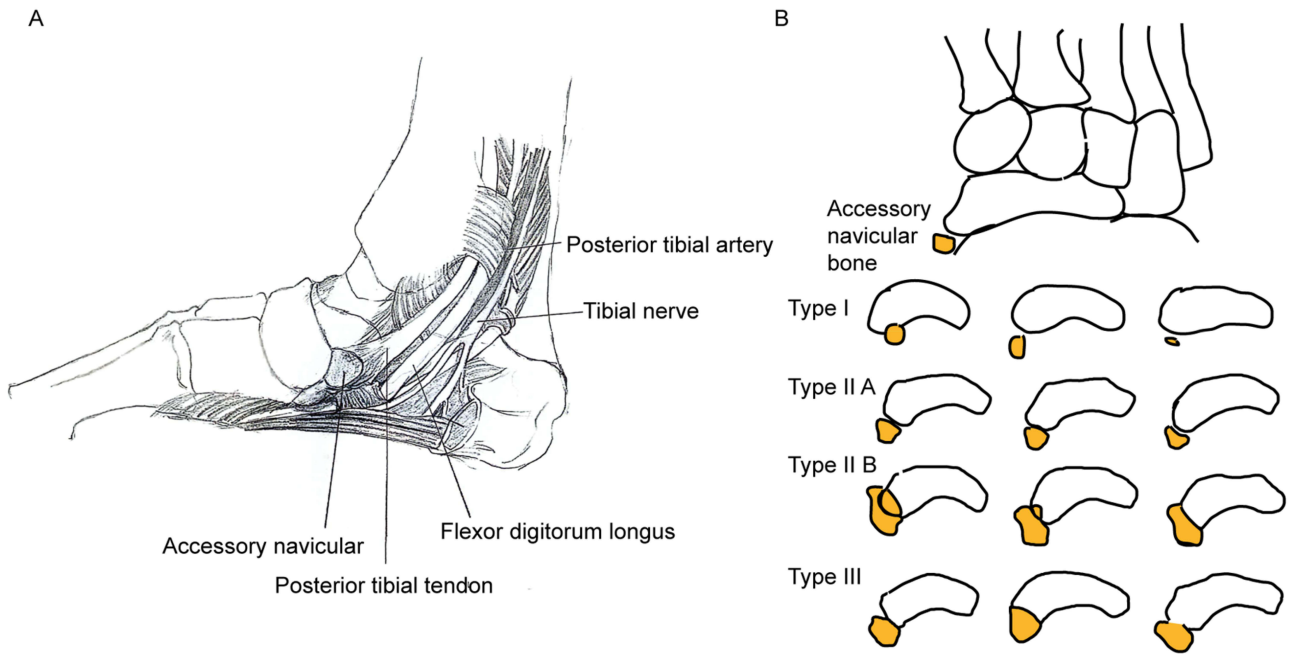

Figure 1 ANB foot anatomy map and subtype classification. (**A**) Schematic diagram of ANB foot anatomy. (**B**) Schematic diagram of ANB subtypes.

Trypsin Digestion

25 mm DTT (Bio-Rad, USA) was used to reduce the protein solution at 37 °C. 60 min later, at room temperature, 50 mm IAA (Bio-Rad, USA) was added to alkylate the solution for 30 min in the dark. Triethylammonium bicarbonate (TEAB) (300 μL) was used to dilute the urea concentration of the protein sample. For the first digestion overnight, trypsin (Promega, USA) was added to the sample (mass ratio, 1:50 trypsin: protein). For the day after, a second digestion was performed.

TMT Quantitative Labeling

The peptides were desalted with an HLB solid phase extraction column (Waters, USA) and vacuum freeze-dried after digestion. After adding 8 μL 5% hydroxylamine, the peptides were labeled with a TMT kit (ThermoFisher Scientific, USA) according to the manufacturer's protocol. NB samples were labeled with TMT tags of 126, 127 N, 127C, 128 N, and 128C, and ANB samples were labeled with TMT tags of 129 N, 129C, 130 N, 130C, and 131. The labeled peptides were mixed, desalted, and dried.

High-Performance Liquid Chromatography (HPLC) Fractionation

The peptide mixtures were fractionated by high-pH reverse-phase HPLC using an XBridge® peptide BEH C18 column. In brief, the peptides were first divided into 40 fractions with a linear gradient of acetonitrile and ddH_2O (pH 10.0) over 51 min. Then, the peptides were combined into 15 fractions and vacuum dried.

Table 1 The Clinical Data for the Patients

Number	Age (years)	Sex	Process (months)	Incidence reason	Foot Imaging Parameters			Pre-Surgical		After Surgery	
					Calcaneal pitch angle	Talar axis-first metatarsal base angle	Arch height (mm)	VAS	AOFAS ankle-hindfoot scale	VAS	AOFAS ankle-hindfoot scale
1	32	Male	24	Athletic training injury	10	15	12	6	49	2	91
2	21	Male	12	Athletic training injury	22	8	13	6	48	2	82
3	21	Male	18	Athletic training injury	24	5	15	4	52	1	90
4	23	Male	11	Athletic training injury	20	13	12	5	49	2	90
5	25	Male	24	Athletic training injury	20	5	13	5	48	1	90

Abbreviations: VAS, Visual Analogue Scale; AOFAS, American Orthopaedic Foot & Ankle Society.

LC-MS/MS Data Analysis

Tryptic peptides were dissolved in solvent A (0.1% formic acid) and separated via a gradient of solvent B (80% acetonitrile and 0.1% formic acid). Separation was performed in the U3000 liquid phase, low pH reversed-phase C18 capillary chromatography. The flow rate was 600 nL/min. The peptides were analyzed by MS/MS using an Orbitrap Q-Exactive-HF-X (Thermo, USA).

Data Analysis

The MS raw data for each sample were searched using the Mascot (version 2.5.1) for identification and quantitation analysis.

Proteomic Analysis

We used the "*t*-test" function in the R (version 3.6) package to identify the DEPs between the ANB and NB groups with $p < 0.05$ & fold change (FC) <0.83 or >1.2. Functional enrichment annotations for DEPs were performed using the Database for Annotation Visualization and Integrated Discovery (DAVID) online tool (https://david.ncifcrf.gov/). The $p < 0.05$ was considered as statistically significant. For Gene Ontology (GO) analyses, enriched biological processes (BPs), molecular functions (MFs), and cellular components (CCs) were assessed. The enrichment degree of the Kyoto Encyclopedia of Genes and Genomes (KEGG) pathway is measured by the rich factor, p-value, and the number of proteins enriched in this pathway. Rich factor refers to the ratio of the number of differentially enriched proteins in the pathway to the number of annotated proteins. In addition, the STRING database (https://string-db.org/) was used to construct the protein-protein interaction (PPI) network with the minimum required interaction score setting to 0.4.

Phosphoproteomics Analysis

Two-dimensional LC-MS identified the phosphorylation site of the protein. The DPPs between the ANB and NB groups were analyzed using the "*t*-test" function in the R package (version 3.6). The thresholds for DPPs were $p < 0.05$ and FC <0.83 or >1.2. KEGG enrichment analysis was performed on DPPs with the screening criteria of $p < 0.05$.

Results

Identification of Proteins

In this study, a total of 2429 proteins were identified, of which 147 DEPs (129 upregulated and 18 downregulated) were quantified between the ANB and NB groups (Figure 2A, Table S1). In addition, the heatmap of the top 100 DEPs was shown in Figure 2B. The top 10 up- and down-regulated DEPs were shown in Table 2.

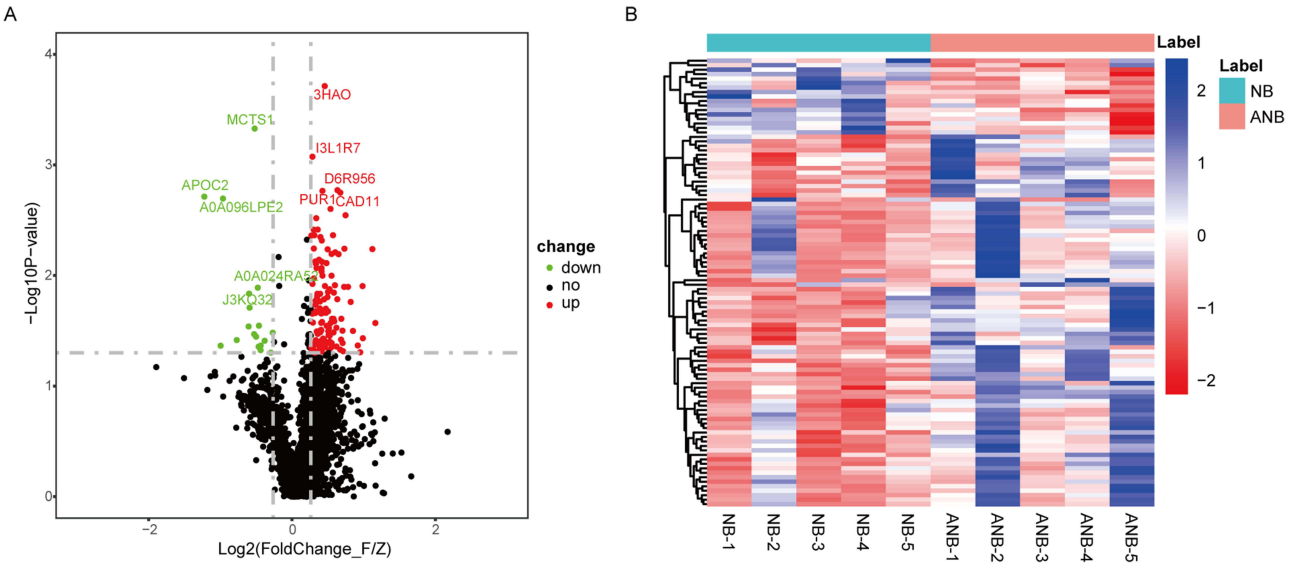

Figure 2 DEPs between the ANB and NB group. (**A**) DEPs were displayed by volcano plots. Red dots represent up-regulated DEPs, and green dots represent down-regulated DEPs. (**B**) DEPs were displayed by Heat map. Changes of the color from blue to red indicate that the DEPs are up-regulated. NB, normal bone; ANB, accessory navicular bone.

Table 2 The Top 10 Up/Down-Regulated DEPs

Protein ID	p-value	Fold change	Regulation	Proteins Name (Gene Symbol)
J3QLE5	0.0268947	2.2388202	up	Small nuclear ribonucleoprotein-associated protein N (Fragment) (SNRPN)
P02462	0.0057685	2.1756668	up	Collagen alpha-1(IV) chain (COL4A1)
H0YAE9	0.0369185	1.9841211	up	Uncharacterized protein (Fragment)
Q9BXX0	0.012466	1.9785209	up	EMILIN-2 OS=Homo sapiens (EMILIN2)
O95865	0.049441	1.9330814	up	Dimethylaminohydrolase 2 (DDAH2)
P47895	0.0429335	1.8887229	up	Aldehyde dehydrogenase family 1 member A3 (ALDH1A3)
A0A7I2V440	0.0317217	1.8025379	up	Cathepsin B OS=Homo sapiens (CTSB)
Q13797	0.0173361	1.7639402	up	Integrin alpha-9 OS=Homo sapiens (ITGA9)
P22897	0.0126703	1.7196152	up	Macrophage mannose receptor 1 (MRC1)
P08572	0.0028517	1.6781766	up	Collagen alpha-2(IV) chain (COL4A2)
P49368	0.0329031	0.829865333	down	T-complex protein 1 subunit gamma (CCT3)
Q9NRX4	0.0498389	0.814794701	down	14 kDa phosphohistidine phosphatase (PHPT1)
P61088	0.0388837	0.767922828	down	Ubiquitin-conjugating enzyme E2 N (UBE2N)
C9JFR7	0.0430233	0.738988218	down	Cytochrome c (Fragment) (CYCS)
P28676	0.0473176	0.738600291	down	Grancalcin OS=Homo sapiens (GCA)
B0YIW2	0.0284303	0.726370704	down	Apolipoprotein C-III (APOC3)
P12429	0.0439912	0.724160807	down	Annexin A3 OS=Homo sapiens (ANXA3)
A0A024RA52	0.0128929	0.71827602	down	Proteasome subunit alpha type (PSMA2)
Q14624	0.0357531	0.706825462	down	Inter-alpha-trypsin inhibitor heavy chain H4 (ITIH4)
Q9ULC4	0.0004692	0.697200524	down	Malignant T-cell-amplified sequence 1 (MCTS1)

Functional Enrichment Analyses of DEPs

GO analyses revealed that these DEPs were enriched in BP terms, such as cell adhesion, cell adhesion mediated by integrin, and cell-matrix adhesion, MF terms, including protein binding, cadherin binding, and integrin binding, and CC terms, including extracellular exosome, cytosol, and extracellular region. The top 10 enriched GO function items were shown in Figure 3A. These DEPs were also enriched in KEGG pathways, including extracellular matrix (ECM)-receptor interaction, focal adhesion, and Cell adhesion molecules (CAMs). The KEGG function enrichment bubble diagram was shown in Figure 3B.

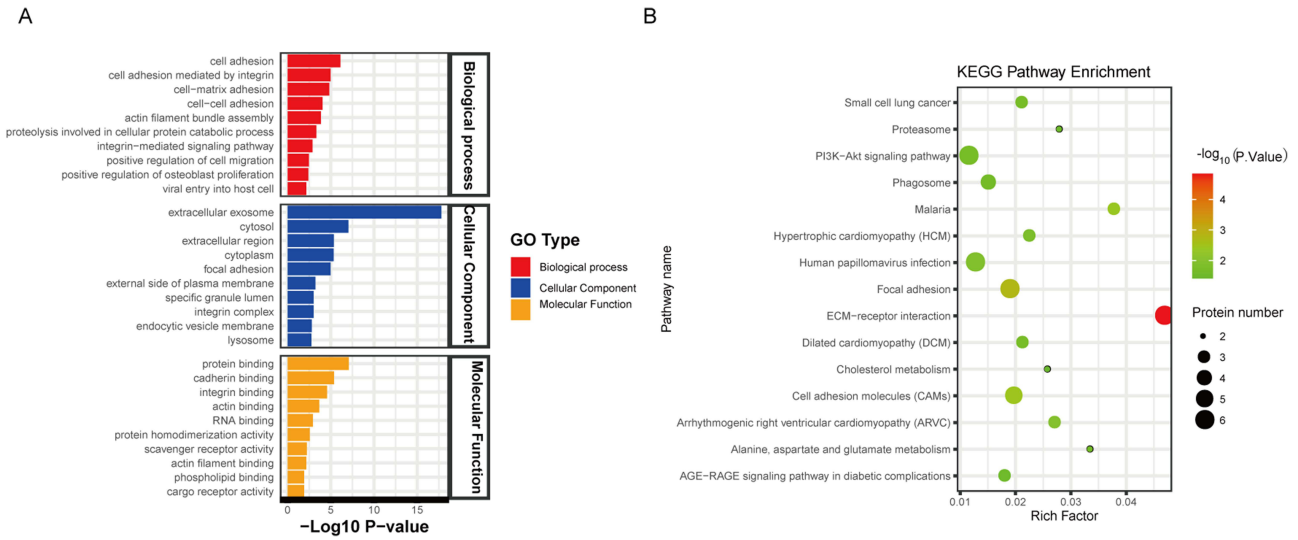

Figure 3 GO and KEGG pathways analysis for DEPs. (**A**) The bar chart showing the top ten biological processes, cellular components, and molecular functions. The vertical axis represents the GO terms, while the horizontal axis indicates the enrichment of DEPs in the corresponding functional terms. The larger of the -log10 P-value, the more correlated between the DEPs and function. (**B**) A bubble chart showing the top 15 KEGG pathways for DEPs. The bubble size represents the number of DEPs, and the bubble color represents the p value.

PPI Network Construction and Hub Gene Identification

The STRING database was next used to construct a PPI network for DEPs (Figure 4). The DEPs ID is compared with the proteins in the STRING database, and the interaction with Confidence score greater than 0.4 was selected to obtain DEPs interaction information. The results showed that the highest interaction score between COL4A1 and COL4A2 was 0.999, followed by RBBP4 and RBBP7 at 0.995.

Identification of Phosphorylation Sites

A total of 251 phosphorylation sites were identified by two-dimensional LC-MS, including 214 class1 phosphorylation sites. Most protein modifications occur on serine (119), followed by threonine (95) and tyrosine (37) (Figure 5A). In most cases, only one phosphorylation modification occurs on a peptide (Figure 5B).

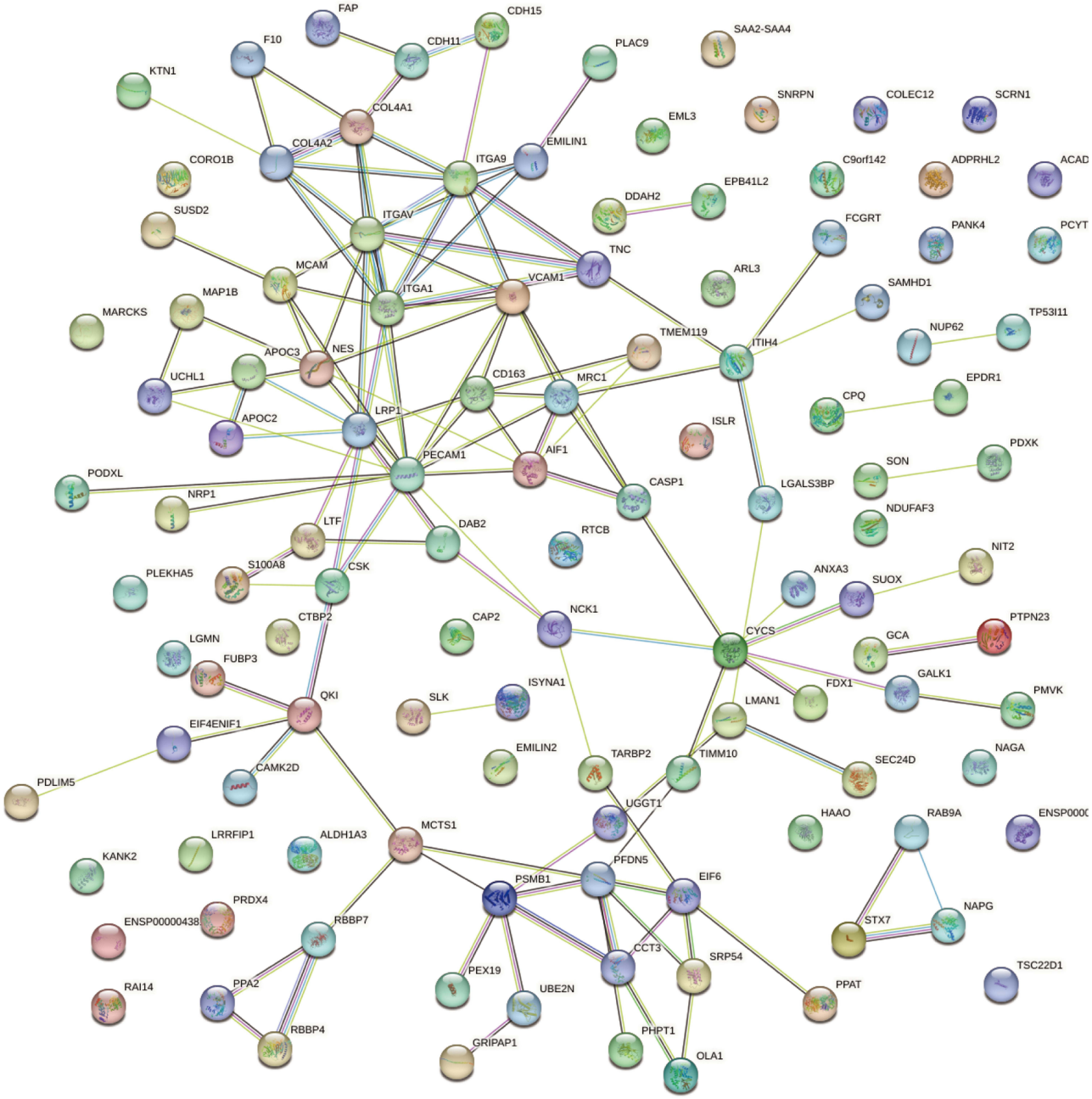

Figure 4 PPI network of DEPs. Nodes in the network represent proteins, lines represent interactions between them, and there is no known interaction between unconnected protein nodes. The wider the line, the higher the score.

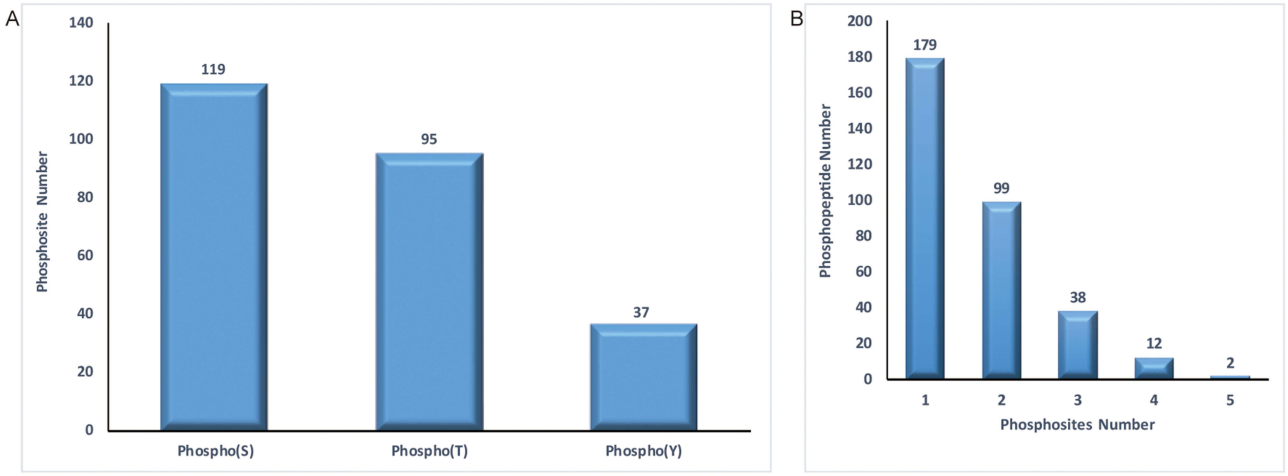

Figure 5 Identified phosphorylation site. (**A**) Bar chart shows the number of phosphorylation sites mainly occurring on three types of amino acids. (**B**) Bar chart shows the relationship between different phosphosites number and the number of phosphopeptides. S, serine; T, threonine; Y, tyrosine.

Identification of DPPs

The "*t*-test" was performed on the quantitative proteins between the ANB and NB groups, and 5 DPPs were identified, of which 4 (BAHD1, JPT1, LIFR, and TESK1) were up-regulated and 1 (PLIN1) was down-regulated (Figure 6A). KEGG analyses revealed that these DPPs were enriched in regulating lipolysis in adipocytes, the PPAR signaling pathway, and signaling pathways regulating the pluripotency of stem cells (Figure 6B). The DPPs were annotated into the pathway map, and the significantly enriched pathway map (hsa04923) is shown in Figure 7.

Discussion

Currently, most studies on ANB concentrate on the diagnosis of patients and evaluation of postoperative prognosis.[4,28] To our knowledge, our research is the first to investigate the proteomics and phosphoproteomics in foot injury with ANB after athletic training. We applied the TMT technology combined with HPLC to qualitative and quantitative proteins to

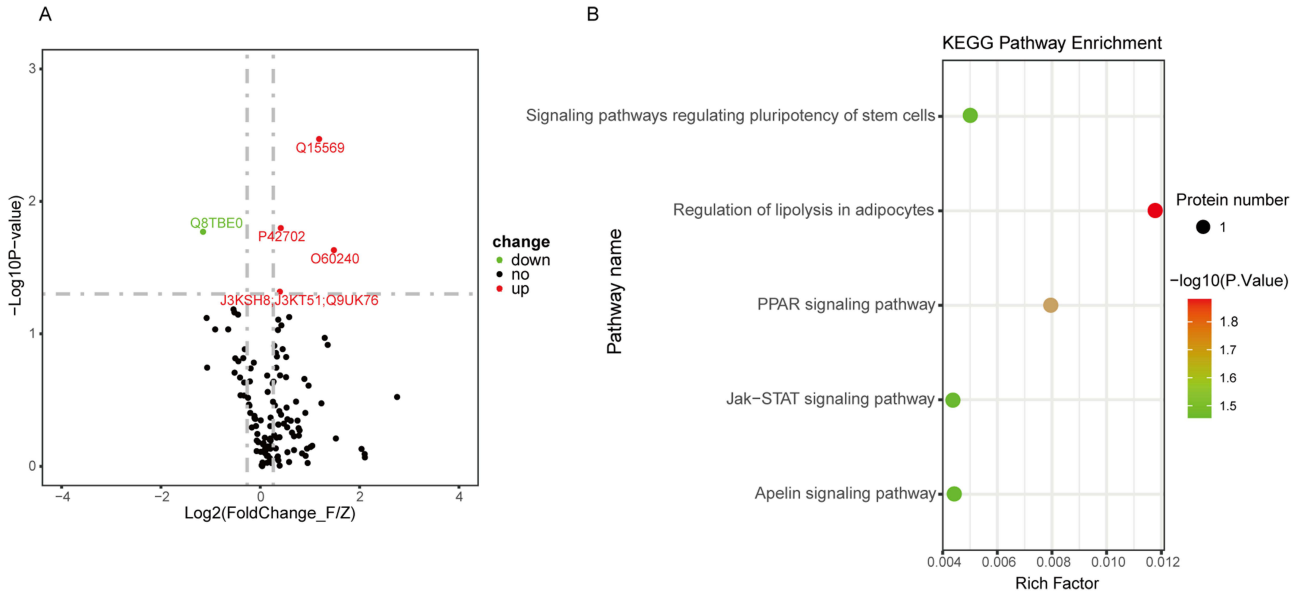

Figure 6 Identification of DPPs between the ANB and NB group and functional enrichment. (**A**) DPPs were displayed by volcano plots. Red dots represent up-regulated DPPs, and green dots represent down-regulated DPPs. (**B**) A bubble chart showing the top 5 KEGG pathways for DPPs. The bubble size represents the number of DPPs, and the bubble color represents the p value.

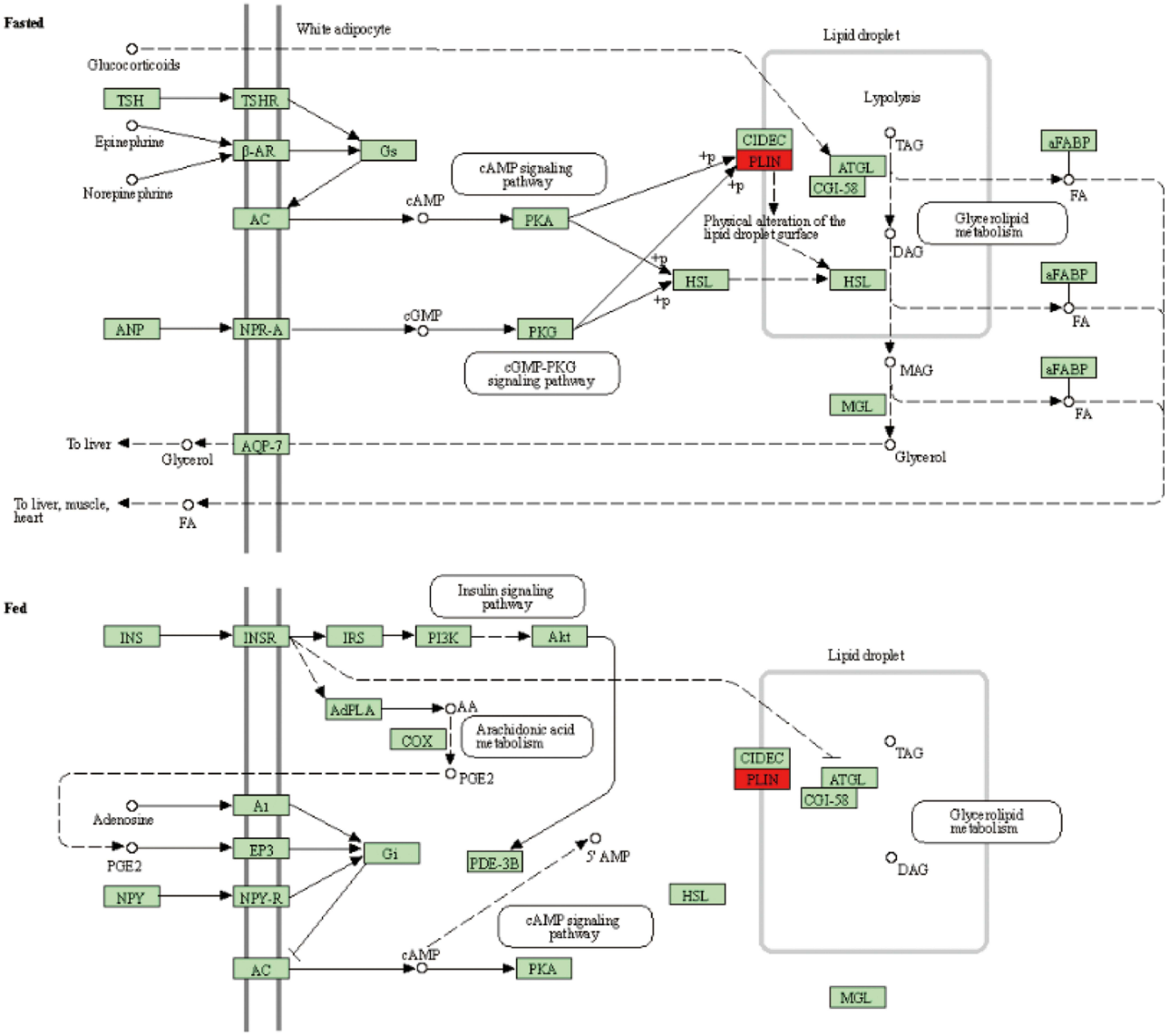

Figure 7 KEGG pathway diagram showing regulation of lipolysis in adipocytes. The red frames represent DPPs and the green frames represent specific genes or enzymes.

identify potential proteins that may be involved in foot injury with ANB after 3 months of athletic training. Moreover, our data may provide more information to understand the underlying mechanism of ANB.

The top 10 up- and down-regulated DEPs represented the most active proteins involved in foot injury with ANB after athletic training. For the top 10 up-regulated DEPs, mainly two distinct function action patterns were exhibited. One (Emilin2, COL4A1, COL4A2, and ITGA9) is associated with repair and regeneration, and the other (MRC1) is linked to inflammatory responses. Extracellular matrix glycoprotein Elastin Microfibril Interfacer 2 (Emilin2) can advance vessel maturation and stabilization in angiogenesis.[29] COL4A1 and COL4A2 are part of the family of type IV collagen α proteins, which play a pivotal role in the process of wound healing.[30] Integrins mediate cell interactions and are critical for osteoblast tissue morphogenesis and architecture.[31] In addition, the Macrophage mannose receptor 1 (MRC1) protein with extremely high expression in foot injury with ANB is mainly involved in inflammatory response.[32] These results indicated that the body's traumatic stress response and immune response process may participate in ANB foot injuries after exercise training, suggesting that MRC1 may be expected to be a therapeutic target to reduce the inflammatory response of ANB foot injury after exercise training.

The top 10 down-regulated DEPs, such as Ubiquitin-conjugating enzyme E2 (UBE2N), Cytochrome c (CYCS), Grancalcin (GCA), and Annexin A3 (ANXA3), were identified in our study. UBE2N plays a vital role in the immune system and holds promise as a therapeutic target for immunological disorders.[33] Inhibition of UBE2N impaired inflammasome activation.[33] Angireddy et al found that dysfunction in cytochrome c oxidase leads to an increase in macrophage phagocytic function and osteoclast formation.[34] The expression of CYCS declined in skeletal muscle aging.[35] GCA can reduce bone turnover and increase fat accumulation in bone marrow.[36] Suppressing ANXA3 can inhibit osteoclast formation via the NF-κB signaling pathway.[37] Therefore, these proteins can provide new directions to further research of foot injury with ANB after athletic training.

The results of function enrichment analysis showed that the DEPs were mainly related to protein binding, extracellular exosomes, cell adhesion, and ECM-receptor interaction. Research has reported that ANB may cause tendon injuries and tibial ankle contusions during athletic training.[10] Exosomes are the key players in facilitating intercellular communication during tissue repair.[38,39] Chamberlain et al showed that exosomes can improve the organization and production of collagen in a rat medial collateral ligament (MCL) injury model.[40] Previous studies showed that one of the critical biological processes is adhesion formation during tendon healing.[41] ECM characteristics have an impact on specific aspects of tissue repair, sports recovery, and risk of reinjury.[42] Based on the findings, it can be inferred that extracellular exosomes and ECM may play a role in foot injury with ANB.

To evaluate the interaction relationships among DEPs, the PPI network was constructed. In the PPI network, COL4A1 has the highest interaction score with COL4A2 (0.999), followed by RBBP4 and RBBP7 (0.995). COL4A1 and COL4A2 form heterotrimers, making them the most abundant and prevalent proteins in basement membranes.[43] In high-intensity intermittent exercise training (HIIT), COL4A1 and COL4A2 may mediate vascular endothelial cell growth and migration via cell adhesion, extracellular matrix organization, and angiogenesis regulation.[44] RBBP4 and RBBP7, which were highly homologous, have essential roles in building and preserving chromatin structure and cell cycle. Xiao et al showed that RBBP4 and RBBP7 serve as compensatory functions in regulating cell growth and apoptosis during the preimplantation of mice embryos.[45] However, the function of COL4A1/COL4A2 and RBBP4/RBBP7 interaction pairs in foot injury with ANB needs to be further investigated in the future.

Perilipin (PLIN1) wraps lipid droplet surface proteins in adipocytes and is highly expressed in adipocytes. Phosphorylation of PLIN1 is crucial for fat metabolism in adipose tissue and adipocyte fat storage.[46] The disorder of lipid metabolites is related to the pathology of rheumatoid arthritis and plays a role in signaling molecules for immune responses.[47] Lipid metabolism is altered in rheumatoid arthritis animal models.[48] Mouse bone marrow-derived mesenchymal stem cells (MSCs) can differentiate into either osteogenic or adipogenic cells.[49] Meyer et al reported that skeletal unloading may change the osteogenic pathway increase marrow adiposity.[49] In our study, the phosphorylation of PLIN1 was significantly increased, and function enrichment analysis revealed significant differences in regulation of lipolysis in adipocytes. However, no significant differences were found in the protein expression level of PLIN1 and the pathways associated with adipocyte proteins in the proteomic results. Whether protein phosphorylation changes its location or structure, or changes the regulatory enzymes activity affect its function is unclear and needs further study.[50] We identified new targets through phosphogenomics that have not been previously discovered in proteomics. Combining the above research results, we speculate that lipid metabolism may be involved in the pathology of foot injury with ANB after athletic training.

Some limitations existed in our research. Due to the rare experimental material, the sample size included in this study was small. Experiments with a larger sample size are likely to reveal more proteins of interest. Further work is required to investigate and validate some DEPs in foot injury with ANB after athletic training. Furthermore, phosphorylation results were obtained based on direct database search analysis of proteome data, which may have limitations in database matching, incomplete phosphorylated peptides signal, and phosphorylation site specificity issues. Therefore, further enrichment of phosphorylated peptides combined with high depth mass spectrometry is needed to improve the accuracy of identification results.

Conclusion

In brief, our study found that foot injury with ANB after athletic training may be associated with proteins related to inflammation and immune system (such as MRC1, UBE2N, CYCS), repair and regeneration system (such as Emilin2, COL4A1, COL4A2, and ITGA9), reducing bone turnover (such as GCA) and inhibiting osteoclasts formation (such as ANXA3). Overall, targeted inhibition of immune inflammatory processes, promotion of tissue repair and regeneration, regulation of bone homeostasis provide scientific guidance and treatment strategies for clinically improving foot injuries caused by ANB after exercise training. These not only enhance our understanding of the pathological process of ANB foot injury, but also lay the foundation for developing new prevention and treatment measures.

Abbreviations

ANB, accessory navicular bone; NB, normal bone; TMT, tandem mass tag; DEPs, differentially expressed proteins; DPPs, differentially phosphorylation proteins; PPI, protein-protein interaction; ECM, extracellular matrix; cAMP, cyclic adenosine monophosphate; PKA, protein kinase A; TEAB, Triethylammonium bicarbonate; HPLC, High Performance Liquid Chromatography; FC, fold change; GO, Gene Ontology; BPs, biological processes; MFs, molecular functions; CCs, cellular components; KEGG, Kyoto Encyclopedia of Genes and Genomes; CAMs, Cell adhesion molecules; Emilin2, Elastin Microfibril Interfacer 2; MRC1, Macrophage mannose receptor 1; UBE2N, Ubiquitin-conjugating enzyme E2; CYCs, Cytochrome c; GCA, Grancalcin; ANXA3, Annexin A3; MCL, medial collateral ligament; HIIT, high-intensity intermittent exercise training; PLIN1, Perilipin; MSCs, mesenchymal stem cells; S, serine; T, threonine; Y, tyrosine.

Data Sharing Statement

The datasets generated during and/or analysed during the current study are available from the corresponding author on reasonable request.

Ethics Approval and Consent to Participate

This study was performed according to the Declaration of Helsinki and approved by the Ethics Committee of Bethune International Peace Hospital (NO. 2023-KY-187). Patients' informed consent was obtained.

Author Contributions

All authors made a significant contribution to the work reported, whether that is in the conception, study design, execution, acquisition of data, analysis and interpretation, or in all these areas; took part in drafting, revising or critically reviewing the article; gave final approval of the version to be published; have agreed on the journal to which the article has been submitted; and agree to be accountable for all aspects of the work.

Disclosure

The authors report no conflicts of interest in this work.

References

1. Huang J, Zhang Y, Ma X, Wang X, Zhang C, Chen L. Accessory navicular bone incidence in Chinese patients: a retrospective analysis of X-rays following trauma or progressive pain onset. *Surg Radiol Anatomy SRA*. 2014;36(2):167–172. doi:10.1007/s00276-013-1158-5
2. Cheong IY, Kang HJ, Ko H, Sung J, Song YM, Hwang JH. Genetic influence on accessory navicular bone in the foot: a Korean twin and family study. *Twin Res Human Genetics*. 2017;20(3):236–241. doi:10.1017/thg.2017.21
3. Lui TH. Endoscopic fusion of the accessory navicular synchondrosis that has no diastasis. *Arthroscopy Tech*. 2017;6(2):e263–e267. doi:10.1016/j.eats.2016.09.029
4. Kara M, Bayram S. Effect of unilateral accessory navicular bone on radiologic parameters of foot. *Foot and Ankle Int*. 2021;42(4):469–475. doi:10.1177/1071100720964820
5. Ray S, Goldberg VM. Surgical treatment of the accessory navicular. *Clin Orthopaedics Related Res*. 1983;(177):61–66.
6. Keles-Celik N, Kose O, Sekerci R, Aytac G, Turan A, Güler F. Accessory ossicles of the foot and ankle: disorders and a review of the literature. *Cureus*. 2017;9(11):e1881. doi:10.7759/cureus.1881

7. Keles Coskun N, Arican RY, Utuk A, Ozcanli H, Sindel T. The incidence of accessory navicular bone types in Turkish subjects. *Surg Radiol Anat*. 2009;31(9):675–679. doi:10.1007/s00276-009-0502-2
8. Scott AT, Sabesan VJ, Saluta JR, Wilson MA, Easley ME. Fusion versus excision of the symptomatic Type II accessory navicular: a prospective study. *Foot and Ankle Int*. 2009;30(1):10–15. doi:10.3113/fai.2009.0010
9. Choi YS, Lee KT, Kang HS, Kim EK. MR imaging findings of painful type II accessory navicular bone: correlation with surgical and pathologic studies. *Korean Journal of Radiology*. 2004;5(4):274–279. doi:10.3348/kjr.2004.5.4.274
10. Wang Y, Tian G, Zhao J, et al. A clinical study of the effect of the paravalvular bone of the foot on military training. *People's Military Surgeon*. 2006;(01):2–4.
11. Kanduc D. The role of proteomics in defining autoimmunity. *Expert Rev Proteomics*. 2021;18(3):177–184. doi:10.1080/14789450.2021.1914595
12. Monti C, Zilocchi M, Colugnat I, Alberio T. Proteomics turns functional. *J Proteomics*. 2019;198:36–44. doi:10.1016/j.jprot.2018.12.012
13. Wang A, Zhang H, Li G, et al. Deciphering core proteins of osteoporosis with iron accumulation by proteomics in human bone. *Front Endocrinol (Lausanne)*. 2022;13:961903. doi:10.3389/fendo.2022.961903
14. Burns J, Wilding CP, Lj R, Hh P. Proteomic research in sarcomas - current status and future opportunities. *Semin Cancer Biol*. 2020;61:56–70. doi:10.1016/j.semcancer.2019.11.003
15. Gong Y, Zou S, Deng D, et al. Loss of RanGAP1 drives chromosome instability and rapid tumorigenesis of osteosarcoma. *Dev. Cell*. 2023;58 (3):192–210e11. doi:10.1016/j.devcel.2022.12.012
16. Huang Y, Liu Y, Huang Q, et al. TMT-based quantitative proteomics analysis of synovial fluid-derived exosomes in inflammatory arthritis. *Front Immunol*. 2022;13:800902. doi:10.3389/fimmu.2022.800902
17. Nielsen RL, Monfeuga T, Kitchen RR, et al. Data-driven identification of predictive risk biomarkers for subgroups of osteoarthritis using interpretable machine learning. *Nat Commun*. 2024;15(1):2817. doi:10.1038/s41467-024-46663-4
18. Hussein AI, Mancini C, Lybrand KE, et al. Serum proteomic assessment of the progression of fracture healing. *J Orthopaedic Res*. 2018;36 (4):1153–1163. doi:10.1002/jor.23754
19. Wei Z, Guo S, Wang H, et al. Comparative proteomic analysis identifies differentially expressed proteins and reveals potential mechanisms of traumatic heterotopic ossification progression. *J Orthop Translat*. 2022;34:42–59. doi:10.1016/j.jot.2022.04.003
20. Guo Y, Yu D, Cupp-Sutton KA, Liu X, Wu S. Optimization of protein-level tandem mass tag (TMT) labeling conditions in complex samples with top-down proteomics. *Anal. Chim. Acta*. 2022;1221:340037. doi:10.1016/j.aca.2022.340037
21. Yang Y, Liu Y, Xia Y, Cheng J, Liu P. Tandem mass tag (TMT) quantitative proteomics and phosphoproteomic of Takifugu rubripes infected with Cryptocaryon irritans. Comparative biochemistry and physiology Part D. *Genomics Proteomics*. 2023;48:101124. doi:10.1016/j.cbd.2023.101124
22. Liang BC, Shi XL, Li CW, et al. Identification of human serum protein targets of Qianggu Decoction in primary type I osteoporosis based on tandem mass tag labeling and liquid chromatography-tandem mass spectrometry technology. *Chin J Integr Med*. 2017;23(10):747–754. doi:10.1007/s11655-016-2600-4
23. Henriques J, Lindorff-Larsen K. Protein dynamics enables phosphorylation of buried residues in Cdk2/Cyclin-a-bound p27. *Biophys J*. 2020;119 (10):2010–2018. doi:10.1016/j.bpj.2020.06.040
24. Olsen JV, Blagoev B, Gnad F, et al. Global, in vivo, and site-specific phosphorylation dynamics in signaling networks. *Cell*. 2006;127(3):635–648. doi:10.1016/j.cell.2006.09.026
25. Shi Y. The investigation of energy metabolism in osteoblasts and osteoclasts. Hua xi kou qiang yi xue za zhi = Huaxi kouqiang yixue zazhi =. *West China J Stomatology*. 2021;39(5):501–509. doi:10.7518/hxkq.2021.05.002
26. Barrio-Hernandez I, Jafari A, Rigbolt KTG, et al. Phosphoproteomic profiling reveals a defined genetic program for osteoblastic lineage commitment of human bone marrow-derived stromal stem cells. *Genome Res*. 2020;30(1):127–137. doi:10.1101/gr.248286.119
27. Olthof MGL, Kempen DHR, Liu X, et al. Bone morphogenetic protein-2 release profile modulates bone formation in phosphorylated hydrogel. *J Tissue Eng Regener Med*. 2018;12(6):1339–1351. doi:10.1002/term.2664
28. Wariach S, Karim K, Sarraj M, Gaber K, Singh A, Kishta W. Assessing the outcomes associated with accessory navicular bone surgery-a systematic review. *Curr Rev Musculoskeletal Med*. 2022;15(5):377–384. doi:10.1007/s12178-022-09772-5
29. Fejza A, Camicia L, Carobolante G, et al. Emilin2 fosters vascular stability by promoting pericyte recruitment. *Matrix Biol*. 2023;122:18–32. doi:10.1016/j.matbio.2023.08.002
30. Oono T, Specks U, Eckes B, et al. Expression of type VI collagen mRNA during wound healing. *J Investigative Dermatol*. 1993;100(3):329–334. doi:10.1111/1523-1747.ep12470022
31. Marie PJ, Haÿ E, Saidak Z. Integrin and cadherin signaling in bone: role and potential therapeutic targets. *Trend Endocrinol Metabol*. 2014;25 (11):567–575. doi:10.1016/j.tem.2014.06.009
32. Matsumoto KI, Aoki H. The roles of tenascins in cardiovascular, inflammatory, and heritable connective tissue diseases. *Front Immunol*. 2020;11:609752. doi:10.3389/fimmu.2020.609752
33. Ni J, Guan C, Liu H, et al. Ubc13 Promotes K63-Linked Polyubiquitination of NLRP3 to Activate Inflammasome. *J Immunol*. 2021;206 (10):2376–2385. doi:10.4049/jimmunol.2001178
34. Angireddy R, Kazmi HR, Srinivasan S, et al. Cytochrome c oxidase dysfunction enhances phagocytic function and osteoclast formation in macrophages. *FASEB j*. 2019;33(8):9167–9181. doi:10.1096/fj.201900010RR
35. Kan J, Hu Y, Ge Y, et al. Declined expressions of vast mitochondria-related genes represented by CYCS and transcription factor ESRRA in skeletal muscle aging. *Bioengineered*. 2021;12(1):3485–3502. doi:10.1080/21655979.2021.1948951
36. Li CJ, Xiao Y, Sun YC, et al. Senescent immune cells release grancalcin to promote skeletal aging. *Cell Metab*. 2021;33(10):1957–1973.e6. doi:10.1016/j.cmet.2021.08.009
37. Lin S, Li M, Zhou Y, et al. Annexin A3 accelerates osteoclast differentiation by promoting the level of RANK and TRAF6. *Bone*. 2023;172:116758. doi:10.1016/j.bone.2023.116758
38. Pan Y, Li Y, Dong W, Jiang B, Yu Y, Chen Y. Role of nano-hydrogels coated exosomes in bone tissue repair. *Front Bioeng Biotechnol*. 2023;11:1167012. doi:10.3389/fbioe.2023.1167012
39. Wan R, Hussain A, Behfar A, Moran SL, Zhao C. The therapeutic potential of exosomes in soft tissue repair and regeneration. *Int J Mol Sci*. 2022;23(7):3869. doi:10.3390/ijms23073869

40. Wang Y, He G, Guo Y, et al. Exosomes from tendon stem cells promote injury tendon healing through balancing synthesis and degradation of the tendon extracellular matrix. *J Cell & Mol Med*. 2019;23(8):5475–5485. doi:10.1111/jcmm.14430
41. Mao WF, Yu YX, Chen C, Wu YF. Transcriptome profiling of digital flexor tendons after injury in a chicken model. *Biosci. Rep.* 2020;40(6). doi:10.1042/bsr20191547
42. Balius R, Alomar X, Pedret C, et al. Role of the extracellular matrix in muscle injuries: histoarchitectural considerations for muscle injuries. *Orthop J Sports Med*. 2018;6(9):2325967118795863. doi:10.1177/2325967118795863
43. Jeanne M, Labelle-Dumais C, Jorgensen J, et al. COL4A2 mutations impair COL4A1 and COL4A2 secretion and cause hemorrhagic stroke. *Am J Hum Genet*. 2012;90(1):91–101. doi:10.1016/j.ajhg.2011.11.022
44. Chen L, Bai J, Li Y. miR-29 mediates exercise-induced skeletal muscle angiogenesis by targeting VEGFA, COL4A1 and COL4A2 via the PI3K/Akt signaling pathway. *Mol Med Rep*. 2020;22(2):661–670. doi:10.3892/mmr.2020.11164
45. Xiao L, Dang Y, Hu B, et al. Overlapping functions of RBBP4 and RBBP7 in regulating cell proliferation and histone H3.3 deposition during mouse preimplantation development. *Epigenetics*. 2022;17(10):1205–1218. doi:10.1080/15592294.2021.1999006
46. Huang P, Le X, Huang F, et al. Discovery of a dual tubulin polymerization and cell division cycle 20 homologue inhibitor via structural modification on Apcin. *J Med Chem*. 2020;63(9):4685–4700. doi:10.1021/acs.jmedchem.9b02097
47. Lei Q, Yang J, Li L, et al. Lipid metabolism and rheumatoid arthritis. *Front Immunol*. 2023;14:1190607. doi:10.3389/fimmu.2023.1190607
48. Srivastava NK, Sharma S, Sinha N, Mandal SK, Sharma D. Abnormal lipid metabolism in a rat model of arthritis: one possible pathway. *Mol Cell Biochem*. 2018;448(1–2):107–124. doi:10.1007/s11010-018-3318-8
49. Meyer MB, Benkusky NA, Sen B, Rubin J, Pike JW. Epigenetic plasticity drives adipogenic and osteogenic differentiation of marrow-derived mesenchymal stem cells. *J Biol Chem*. 2016;291(34):17829–17847. doi:10.1074/jbc.M116.736538
50. Sharma K, D'Souza RC, Tyanova S, et al. Ultradeep human phosphoproteome reveals a distinct regulatory nature of Tyr and Ser/Thr-based signaling. *Cell Rep*. 2014;8(5):1583–1594. doi:10.1016/j.celrep.2014.07.036